



Synthesis of highly branched sulfonated polymers and the effects of degree of branching on properties of branched sulfonated polymers as proton exchange membranes



Huixiong Xie, Duan Wang, Dan Tao, Lei Wang*

Shenzhen Key Laboratory of Special Functional Materials, College of Materials Science and Engineering, Shenzhen University, Shenzhen 518060, China

HIGHLIGHTS

- The branched polymer with 10% branching agent was synthesized.
- The membrane exhibits considerable proton conductivity and oxidative stability.
- A₂ with hindrance and B₃ with long and hard arms can increase degree of branching.
- The microstructure of the branched membrane was investigated by SEM and AFM.

ARTICLE INFO

Article history:

Received 23 November 2013

Received in revised form

14 March 2014

Accepted 17 March 2014

Available online 12 April 2014

Keywords:

Branched polymer

Poly(arylene ether)s

Oxidative stability

Proton exchange membrane

Fuel cells

ABSTRACT

Branched sulfonated polymers exhibit excellent properties as proton exchange membranes (PEMs). However, very few highly branched sulfonated polymers are reported as PEMs. The highly branched polymer, including the method to increase degree of branching (DB) and the effects of DB on the properties of PEMs, should be further studied. In this work, novel branched sulfonated poly(fluorenyl ether ketone sulfone)s with different DB value are synthesized by direct polycondensation reactions from bisphenol fluorene (A₂), sulfonated 4,4'-difluorobenzophenone, 1,3,5-tris(4-(4-fluorophenylsulfonyl)phenyl)benzene (B₃-3) and 4,4'-difluorodiphenyl sulfone. The highest DB with 10% branching agent is obtained using the B₃-3 monomer. The method to increase the DB is discussed. It is found that B₃ scaffold with long and hard arms can effectively increase the DB value. The effects of DB on the properties, including oxidative stability, proton conductivity, water uptake, swelling ratio, thermal stability, mechanical property and microstructure, are investigated. With increasing DB value, oxidative stability and proton conductivity of the membranes increase remarkably, but swelling ratio and tensile strength decrease slowly. The membrane with the highest DB value (10%) exhibits high proton conductivity (0.42 S cm⁻¹) and oxidative stability (327 min), as well as relatively low swelling ratio (16.2%) at 80 °C.

© 2014 Elsevier B.V. All rights reserved.

1. Introduction

Proton exchange membrane fuel cells (PEMFCs) have received worldwide attention due to their potential applications in portable and stationary power generation, personal electronic devices and automobiles [1–3]. One of the main barriers to the commercial introduction of PEMFCs is the lack of membranes [4]. Although a considerable progress has been made on the development of proton exchange membranes (PEMs) in the past few years [5–7], the durability and cost are still two major obstacles hindering widespread application [8,9]. Perfluorosulfonic acid PEMs, such as

Nafion membrane, are typically used as the polymer electrolytes in PEMFCs because of their high proton conductivity, excellent chemical and oxidative stability. However, high cost is a major obstacle for their widespread application in PEMFCs. The modification of Nafion is very difficult to reduce the cost since the modified membrane has a major content of Nafion [9]. The cheaper, usually fluorine-free, alternative acid-functionalized aromatic hydrocarbon-based polymers were found to possess good thermal stability, appropriate mechanical strength and high proton conductivity [10]. However, most of them failed to be used as proton exchange membranes since their short lifetime due to a combination of hydrolysis and oxidative degradation [11,12]. Therefore, to improve the durability of the inexpensive membranes becomes an active area of research on PEMs [8,13–15].

* Corresponding author.

E-mail address: wl@szu.edu.cn (L. Wang).

Among the inexpensive membranes, the membranes cast from sulfonated poly(arylene ether)s [10,16–18] have drawn increasing attention owing to their excellent properties such as high proton conductivity, good heat resistance and low methanol diffusion. The membranes could be potentially used as PEMs if their durability can meet the requirements of fuel cell. Therefore, extensive efforts have been made to improve the durability of the membranes [17,19–24], among which cross-linking is an effective way [25,26]. Various cross-linked PEMs have been reported [7,27–30]. Na et al. prepared a series of cross-linked hybrid membranes by a combination of silane-crosslinking and thiolene click chemistry based on a sulfonated poly(arylene ether ketone), which exhibited high dimensional stabilities and high oxidative stabilities [31]. Chen et al. reported a series of quinoxaline-based crosslinked membranes with excellent oxidative stabilities and the elapsed time of the crosslinked membranes was 2–3 times longer than that of the corresponding precursor membranes in Fenton's reagent [32]. However, the cross-linked membranes are usually insoluble in common organic solvents and difficult to reprocess.

Compared to cross-linked PEMs, branched PEMs, not only can effectively improve oxidative stability and conductivity, but also have good solubility in common organic solvents. However, up to now only a few branched PEMs have been reported [33–38]. Hay et al. [34] reported branched poly(arylene ether)s with sulfonic acid groups on the end groups. At the same level of IEC as Nafion, the branched PEMs showed proton conductivities comparable to that of Nafion. The resultant membranes have good oxidative stability because of the low IEC value. Unfortunately, their structures are limited in terms of number of sulfonated units because the number of terminated groups is only 2 or 3 per molecule. Ueda et al. [33] have developed a series of sulfonated block copolymers with hydrophilic and hydrophobic segments as arms, which exhibited high oxidative stability. The design of structure is ingenious, but it is difficult to synthesis. Park et al. [35] have prepared a series of branched sulfonated polymers containing branching agent lower than 0.4% by a facile method. The resultant polymers had a positive effect on the oxidative stability and mechanical strength. However, when the branching agent was increased to higher than 0.4%, the polymers were cross-linked by itself during the polymerization and thus the highly branched polymers could not be obtained. In order to obtain highly branched fluorine-free polymers, Our group has introduced 1,1,1-tris(4-hydroxyphenyl) ethane [39] (B_3-1) and 1,3,5-tris[4-(4-fluorobenzoyl)phenoxy]benzene [40] (B_3-2) as the branching agents to synthesize two series of branched non-fluorinated polymers, and the DB value was 2% and 4%, respectively. The structure of B_3 was showed in Fig. 1. This suggests that

appropriate branching agent can effectively increase DB value. The synthesized branched nonfluorinated polymers with 4% DB value exhibited better oxidative stability and proton conductivity than those with 2% DB value. Recently, Wang et al. [37] successfully prepared partially fluorinated branched sulfonated poly(ether ether ketone)s by introducing 1,3,5-tris(4-fluorobenzoyl)benzene as the branching agent. The highest DB value was 6.67%. The membrane prepared by the branched polymer showed better oxidative stability than those with 4% DB value reported by our group [40]. All of these inspire us to go to prepare a novel branched sulfonated polymer with higher DB by special design of B_3 structure.

In this paper, 1,3,5-tris(4-(4-fluorophenyl sulfonyl)phenyl)benzene (B_3-3) was selected as the branching agent. The special B_3 structure with longer and harder arms are believed to further reduce the cross-linked opportunities of the branched polymers and increase DB value. Therefore, a series of novel branched non-fluorinated sulfonated poly(fluorenyl ether ketone sulfone)s with different DB value (0%–10%) were synthesized. The method to increase the DB value and the effects of DB on the properties, including hydrolysis and oxidative stabilities, ion-exchange capacity (IEC), proton conductivity, water uptake, thermal stability, swelling ratio and microstructure of the membranes, were investigated.

2. Experimental

2.1. Materials

1,3,5-Triphenylbenzene, 4,4'-difluorodiphenyl sulfone (DFDS), 4-fluorobenzenesulfonyl chloride, Sulfonated 4,4'-difluorobenzophenone (SDFBP) and bisphenol fluorene were purchased from commercial sources and used as received. Toluene was dried with sodium wire and DMAC was dried with 4 Å molecule sieves prior to use. Anhydrous potassium carbonate was dried at 300 °C for 24 h in furnace prior to use.

2.2. Measurement

^1H NMR spectra, reported in ppm, were recorded on a Varian 400-Hz NMR instrument using DMSO- d_6 as solvent and tetramethylsilane (TMS) as the internal standard. Inherent viscosities of the polymer solutions of $\sim 0.5 \text{ g dL}^{-1}$ concentration in DMAC were measured using an Ubbelohde viscosity meter at 30 °C. Glass transition temperatures (T_g) were determined on a TA instrument Q200 DSC at a heating rate of 10 °C min^{-1} under the protection of

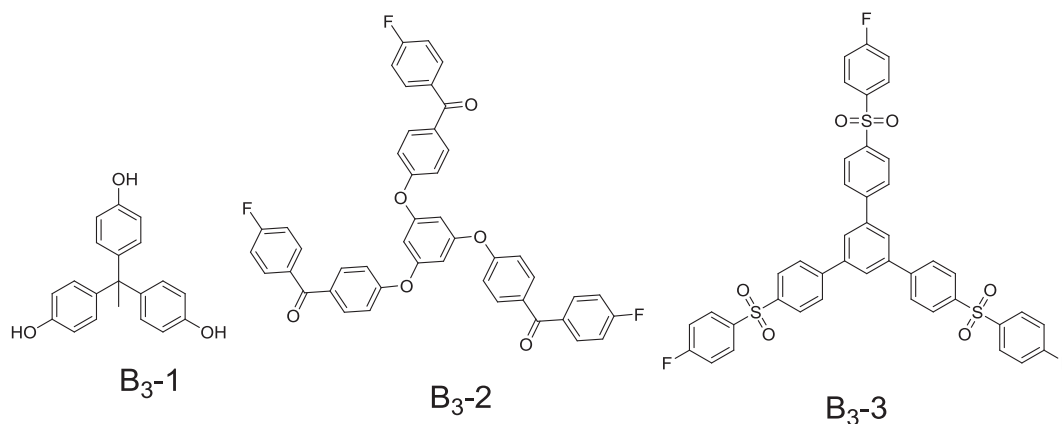


Fig. 1. Structures of B_3 monomers.

nitrogen. The second scan was immediately initiated just after the sample was cooled to room temperature. Thermal stability of the polymers was investigated on a Q50 TGA instrument at a heating rate of $10\text{ }^{\circ}\text{C min}^{-1}$ in the temperature range from 30 to $600\text{ }^{\circ}\text{C}$ under a nitrogen environment with a flow of 50 mL min^{-1} .

2.3. Synthesis of 1,3,5-tris[4-(4-fluorophenyl sulfonyl)phenoxy]benzene (**B₃-3**)

The **B₃-3** was synthesized from 1,3,5-triphenylbenzene and 4-fluorobenzenesulfonyl chloride using the method reported in the literature [34]. A white powder was obtained in overall 75.9% yield, after purified by recrystallization from acetic acid. The structure of **B₃-3** was confirmed by $^1\text{H NMR}$. $^1\text{H NMR}$ (CDCl_3 , ppm): 7.22–7.30 (m, 6H), 7.78–7.81 (m, 9H), 8.02–8.08 (m, 12H). Mp: 143–144 $^{\circ}\text{C}$.

2.4. Synthesis of linear polymers **5**

Linear sulfonated poly(arylene ether) **5** was synthesized by reaction of bisphenol fluorine (0.70 g, 2.0 mmol), 4,4'-difluorodiphenyl sulfone (0.2032 g, 0.8 mmol) sulfonated difluorobenzophenone (0.5064 g, 1.2 mmol) using a modified method reported in the literature [39]. The fibrous polymer **5** was collected and dried at $110\text{ }^{\circ}\text{C}$ under vacuum for 24 h (yield: 94%).

$^1\text{H NMR}$ (400 MHz, DMSO, ppm): 8.16 (s, 0.6H), 7.84–7.92 (m, 1.8H), 7.60 (d, 0.6H), 7.35–7.47 (m, 3H), 7.15 (m, 2H), 7.04 (d, 0.8), 6.95 (d, 2H), 6.84 (d, 0.6H).

2.5. Synthesis of the branched polymers **6a–f**

As shown in Scheme 1, the branched sulfonated poly(aryl ether) **s 6a–f** were successfully synthesized. The polymerization procedure for the polymer **6f**, a typical example for synthesis of the branched polymers **6a–f**, is described below. The bisphenol fluorine (1.40 g, 4.00 mmol), sulfonated difluorobenzophenone (1.0128 g, 2.40 mmol), DFDS (0.254 g, 1.00 mmol), **B₃-3** (0.3124 g, 0.40 mmol), potassium carbonate (0.8278 g, 6.0 mmol), DMAc (10 mL) and toluene (10 mL) were carefully introduced into a 50 mL three-neck round bottom flask equipped with a Dean–Stark trap and condenser under nitrogen protection. Toluene was used as azeotropic solvent to remove the water formed during the reaction. The reaction mixture was kept at $140\text{ }^{\circ}\text{C}$ for 4.0 h to remove the water produced and then heated to $170\text{ }^{\circ}\text{C}$ (oil bath temperature) to distill the toluene off. The reaction mixture was kept at this temperature for 4 h. After cooled, the resulting viscous mixture was diluted with 5 mL DMAc and poured slowly into 100 mL of the mixture of deionized water and methanol containing 2 mL of concentrated HCl to precipitate the formed polymer. The precipitates were filtered and washed with water for three times to remove inorganic salts. The fibrous polymer was collected and dried at $110\text{ }^{\circ}\text{C}$ under vacuum for 24 h (Yield: 91.2%).

$^1\text{H NMR}$ (400 MHz, DMSO, ppm): 8.14 (s, 0.6H), 8.04 (br, 0.3H), 7.84–7.96 (m, 2.1H), 7.60 (d, 0.6H), 7.34–7.49 (m, 3.0H), 7.15 (m, 2H), 7.04 (d, 0.5H), 6.95 (d, 2H), 6.84 (d, 0.6H).

2.6. Film casting and membrane acidification

The salt form of linear and branched polymers were dissolved in 10 mL DMAc by stirring at room temperature and filtered through a funnel. The filtration was cast on the glass slides and dried under vacuum at $60\text{ }^{\circ}\text{C}$ for 24 h to obtain the tough and smooth membranes. The resultant membranes were acidified with 2 M HCl solution for 24 h to exchange Na^+ ions with H^+ ions. Finally, the membranes were immersed in deionized water overnight to get rid of excessive HCl and kept in deionized water for testing purposes.

2.7. Water uptake, dimensional stability and ion-exchange capacity

After immersed in deionized water at $30\text{ }^{\circ}\text{C}$ for more than 8 h, the films were taken out, wiped, dried and quickly weighed. The water uptake (WU, wt %) was calculated by the following equation:

$$\text{WU} = (W_s - W_d)/W_d \times 100\%$$

where W_s is the weights of the wet membranes obtained at different temperatures; W_d is the weights of the dry membranes obtained by weighting the dry films dried at $110\text{ }^{\circ}\text{C}$ under vacuum for 24 h.

Dimensional change was investigated by immersing the membrane into water at different temperature for 24 h. The change of length was calculated from the equation:

$$\text{Swelling ratio}(\%) = (L_s - L_d)/L_d \times 100\%$$

where L_s and L_d are the length of wet and dry membrane, respectively.

Ion-exchange capacity (IEC) of the membranes was measured by titration. The membranes were first converted to acid form and immersed in a 2 M NaCl solution for 24 h to exchange H^+ ions with Na^+ ions. Then, the exchanged H^+ ions within the solutions were titrated with a 0.01 M NaOH solution using phenolphthalein as an indicator. The IEC values were calculated according to the following equation:

$$\text{IEC}(\text{m eq g}^{-1}) = (M_{\text{NaOH}} \times V_{\text{NaOH}})/W_d$$

where M_{NaOH} and V_{NaOH} stand for the molar concentration and volume (mL) of the aqueous NaOH solution used in titration and W_d (g) is the weight of dry membrane.

2.8. Proton conductivity

Proton conductivity measurement was conducted on the hydrated film using an impedance analyzer (Solartron 1260A) with an oscillating voltage of 10 mV and frequency range from 10 MHz to 500 Hz. Prior to the measurement, the membrane was immersed in 1 M H_2SO_4 at room temperature for 24 h and then washed to a pH of 7 with deionized water. After kept in deionized water over 12 h, the membrane was tightly clamped and placed in a closed container with the relative humidity of 100%. The whole container was placed in a temperature-controlled water bath during the measurement. The proton conductivity was calculated from the impedance data according to following equation:

$$\sigma = d/RS$$

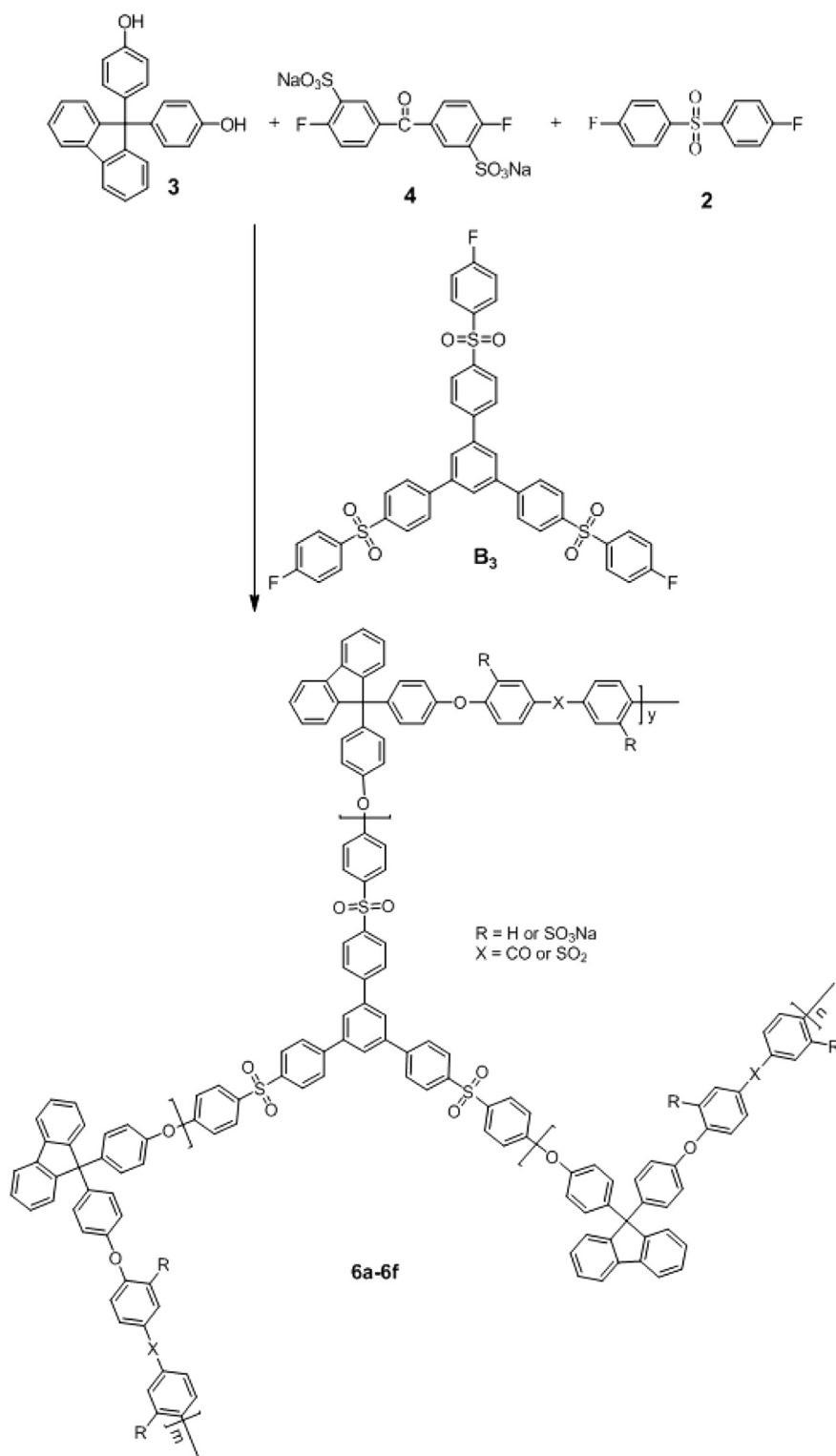
where d and S are the thickness and the cross-sectional area of the specimen, respectively, and R is the membrane resistance measured by impedance analyzer.

2.9. Oxidative stabilities and hydrolytic stabilities

The oxidative stability was investigated by immersing the membranes into Fenton's reagent (2 ppm FeSO_4 in 3% H_2O_2) at $80\text{ }^{\circ}\text{C}$. The oxidative stability of the membranes was characterized by the expended time that the membranes started to break into pieces. The hydrolytic stability was also investigated by treating membrane samples in boiling water.

2.10. Hydration number (λ), membrane density and AFM

The hydration number (λ) indicates the number of water molecules absorbed per sulfonic acid group and is calculated by



Scheme 1. Synthesis of branched polymers **6a–f**.

combining water uptake and IEC data. Using the dry (W_d) and the wet (W_s) membrane weights, λ were calculated as follows:

$$\lambda = [(W_s - W_d)/18] \times 1000 / (W_d \times \text{IEC}) = (WU \times 1000) /$$

Membrane density was calculated from measurements of

membrane dimensions and weight after drying at 110 °C for 24 h according to the method reported by the literature [41].

The microscopic morphology of membranes was investigated by an atomic force microscope (AFM) using a Dimension Icon Scanning Probe Microscope.

3. Results and discussion

3.1. The method to increase DB value

Park et al. reported branched sulfonated poly(arylene ether ketone)s (Polymer 7) containing 0.4 mol% B₃-1 with good oxidative stability and mechanical strength by facile method [35]. The branched sulfonated poly(ether ketone) (Polymer 8) containing 2 mol% B₃-1 and the branched sulfonated polymers (Polymer 9) containing 4 mol% B₃-2 were synthesized by our group [39,40]. The structures of the branched polymers were depicted in Fig. 2. From comparing the Polymer 7 and Polymer 8, we can see that introducing the fluorene ring is a very effective way to improve the degree of branching. The fluorene ring in the branched polymers with large steric hindrance makes the polymer chain more difficult to close, leading to reducing cross-linked opportunities of the branched polymer, and thus to improve the degree of branching. The results indicate that the A₂ monomer with larger steric hindrance can significantly improve the DB value. From the polymers 8 and 9, it is found that the polymers with different DB values are obtained by different B₃ monomers. It can be inferred that the structure of B₃ is also an important factor to affect the degree of branching. Contrasting the monomers, B₃-1 and B₃-2, we can see that the B₃ scaffold with long and hard arms can reduce cross-linked opportunities of the branched polymers and improve the degree of branching. In this work, both 1,3,5-tris[4-(4-fluorophenylsulfonyl)phenoxy]benzene with longer and harder arms (B₃-3) and bisphenol fluorene with the large steric hindrance fluorene ring (A₂) are introduced into the branched polymers. A

series of novel branched sulfonated poly (fluorenyl ether ketone sulfone)s with different DB value were designed.

3.2. Synthesis of the polymer membranes

The B₃-3 was synthesized using 1,3,5-triphenylbenzene and 4-fluorobenzenesulfonyl chloride. The structure of B₃-3 was confirmed by ¹H NMR, and the signals of B₃-3 were observed at 7.22–7.30 ppm, 7.78–7.81 ppm, 8.02–8.08 ppm, respectively. The linear and branched sulfonated nonfluorinated poly(arylene ether)s were synthesized by a reaction of bisphenol fluorene, sulfonated 4,4'-difluorobenzophenone, 4,4'-difluorodiphenyl sulfone and B₃-3 in the presence of potassium carbonate in a DMAc/toluene solvent system. In order to obtain high performance membranes, the sulfonated polymer composition was set at 60% (using 60 mol% of sulfonated difluorobenzophenone relative to mol% of bisphenol fluorene employed). The polymerization was studied by changing the amounts of B₃ from 3.33 mol% to 12 mol% relative to mol% of bisphenol fluorene employed. When the amount of B₃-3 was over 10 mol%, the branched polymers were easily crosslinked during the polymerization and became insoluble in polar solvents.

As shown in Table 1, all the polymers have high yields and reasonably high intrinsic viscosities. These high intrinsic viscosities indicate that all the polymers exhibit high molecular weight and can be cast into transparent, flexible, and tough membranes. The branched polymer **6f** was selected for analyzing chemical structure by ¹H NMR spectroscopy as an example. The ¹H NMR spectra of the linear polymer **5** and the branched polymer **6f** are shown in Fig. 3. As compared with the linear polymer **5**, a new peak at about

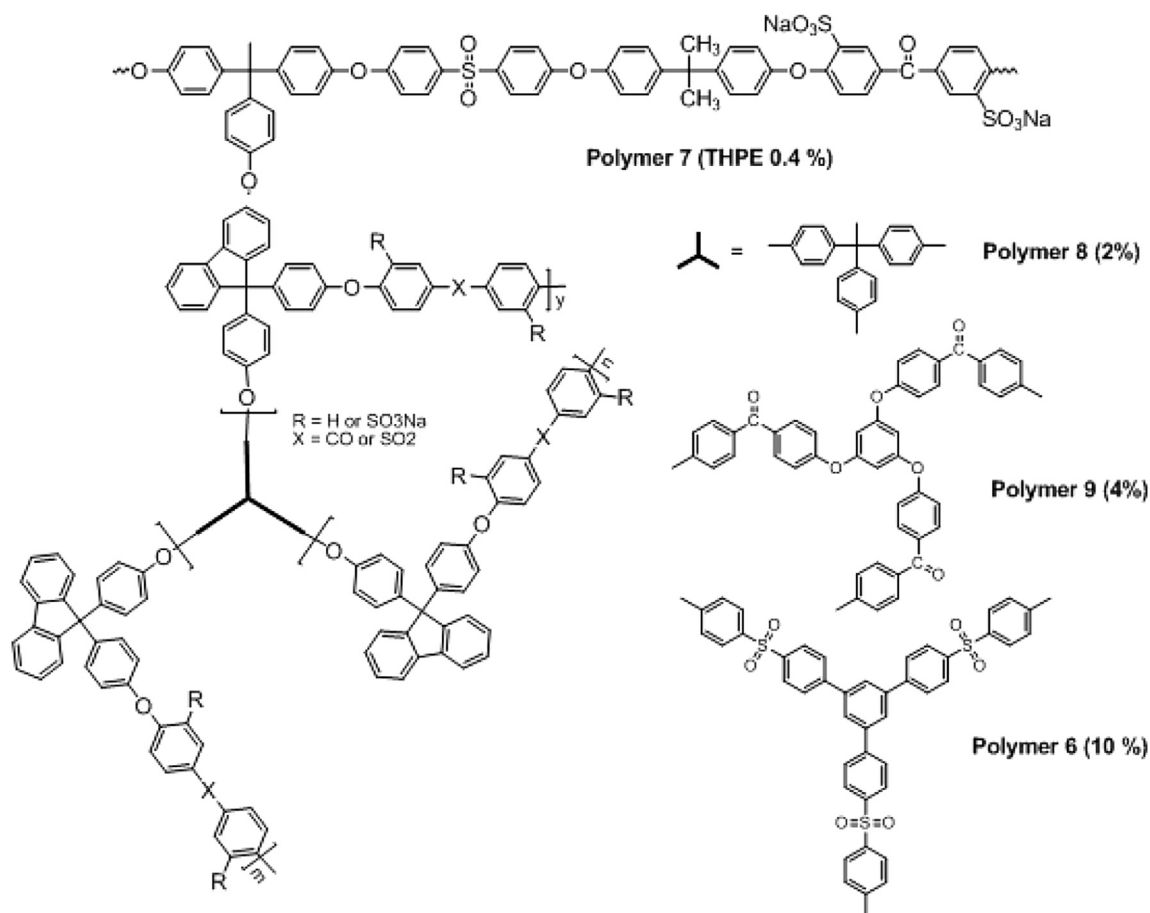


Fig. 2. Structures of branched polymer **6f** and polymers **7–9**.

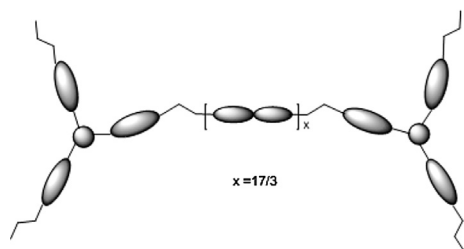
Table 1
Properties of polymer **5** and branched polymers **6a–f**.

	B ₃ -3 (%)	Yield (%)	η_{inh}^a (dLg ⁻¹)	IEC ^b (meqg ⁻¹)	IEC ^c (meqg ⁻¹)	Conductivity ^d (10 ⁻² S cm ⁻¹)	Oxidation stability (min)
5	0	92	0.99	1.88	1.83	1.78	100
6a	3.33	93	0.77	1.84	1.80	15.93	255
6b	4.67	91	0.86	1.82	1.77	20.90	269
6c	6.00	94	1.35	1.81	1.77	25.96	281
6d	7.33	92	1.39	1.80	1.74	34.00	292
6e	8.67	94	1.68	1.78	1.72	39.89	312
6f	10.00	91	2.85	1.77	1.71	42.15	327
Nafion 117	—	—	—	0.91	0.91	10.08	>400

^a Measured at 30 °C in DMAC.^b The theoretical IEC.^c The experimental IEC.^d Measured at 80 °C and 100% relative humidity for hydrate membrane samples.

8.04 ppm was found in the **6f**. The peak at about 7.87 ppm increases while the peak at about 7.05 ppm decreases in **6f**. The decrease of the peak at about 7.05 ppm is due to the decrease of the DFDS feed amount. The increase of the peak at about 7.87 ppm and the occurrence of the new peak at about 8.04 ppm suggest that the B₃ moiety is introduced into the copolymers. The polymers containing 3.33–10% B₃-3 showed good solubility, as listed in Table 2. The linear and the branched polymers are soluble in polar organic solvents, such as NMP, DMAC, DMSO, DMF, insoluble in H₂O and CH₃OH, and can be readily cast from DMAC solutions to form tough and smooth films.

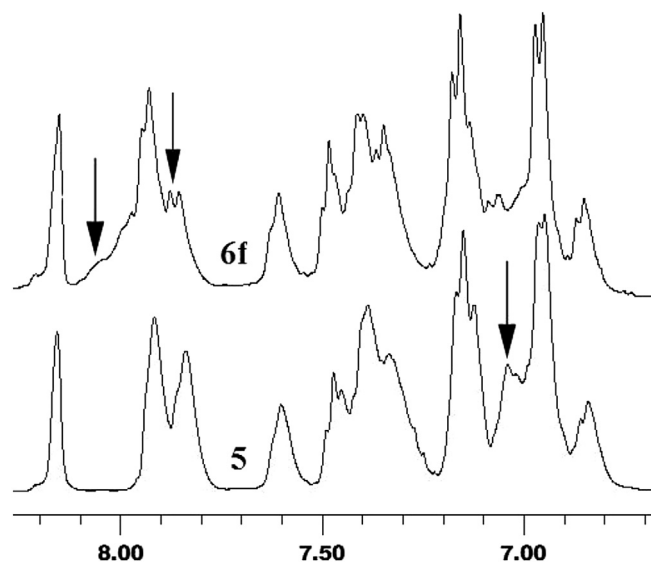
The composition of the branched polymer **6f** is analyzed, which is shown in Scheme 1. When the degree of branching is 10%, 15% bisphenol fluorine is reacted with B₃. The ratio of B₃ and the repeating units ($m + n + y$) is 1: 8.5. The average units in each arm are 8.5/3 and the average units between the branching points are about 17/3. The short chain between the branching points may decrease the chain entanglement and affects the properties of the branched membranes. The diagram is as follows.



3.3. Ion-exchange capacity, water uptake and dimensional stability

IEC is an important parameter for evaluation of a PEM as it influences the water uptake and proton conductivity. The IEC values of the linear and branched polymers are presented in Table 1. The theoretical IEC values were calculated from the polymer molecular formula, while the experimental values were measured by titration. The IEC values slightly decreased with increasing DB value. The experimental IEC values are agreement with the theoretic values. This indicated that the sulfonate groups were successfully incorporated into the polymer backbones via sulfonated monomer copolymerization without any side reactions.

Water uptake (wt %) of the sulfonated polymer membranes was measured at different temperatures under immersed conditions in deionized water. The results are shown in Fig. 4. Compared with the linear membranes, the branched membranes exhibit higher water uptake. With increasing DB value, the water uptake of the branched

**Fig. 3.** ¹H NMR spectra of polymer **5** and branched polymer **6f**.

polymer membranes increases significantly. The amount of water uptake in the membranes is strongly dependent on the amount of sulfonic acid groups and is also related to IEC values. Generally, a higher sulfonation level leads to greater IEC value and in turn results in higher water uptake. However, with decreasing IEC values, water uptake of the branched polymer membranes increases significantly. We infer that the results can mainly be attributed to the introduction of branching points. It is believed that different domains in linear polymer membranes can be formed by micro-phase separation due to the mutual repulsion between hydrophilic sulfonate groups and hydrophobic blocks, and water molecules mainly aggregated near the hydrophilic sulfonate groups. The hydrophobic regions in linear polymer membrane are difficult to absorb water. However, the branched polymer membranes are different and water can filter into the hydrophobic region in the three-dimensional structure near the branching points, which might contribute to the high water uptake of the branched polymers.

In order to evaluate the dimensional stability of the membranes, the swelling ratio of the branched membranes was characterized at different temperature by comparing their hydrated state with their dry state. The results are shown in Fig. 5. Compared with the linear membrane, the branched membranes exhibited better dimensional stability. The swelling ratio of the branched membranes decreases with increasing DB value. In general, the water uptake of PEM influences dimensional stability and excessive water uptake can deteriorate the dimensional stability, even leading to high swelling and solubility. However, the branched membranes exhibit special

Table 2
Solubility of polymer **5** and branched polymers **6a–f**.

	DMAC	DMSO	DMF	NMP	H ₂ O	CH ₃ OH
5	+ ^a	+	+	+	— ^b	—
6a	+	+	+	+	—	—
6b	+	+	+	+	—	—
6c	+	+	+	+	—	—
6d	+	+	+	+	—	—
6e	+	+	+	+	—	—
6f	+	+	+	+	—	—

^a +, soluble.^b —, insoluble.

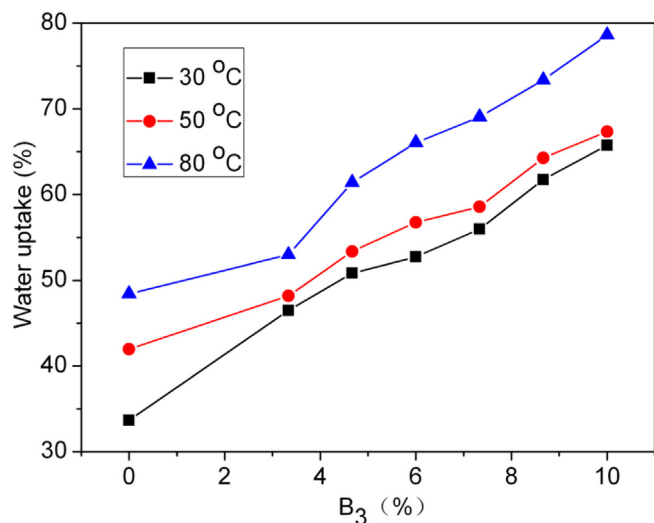


Fig. 4. Water uptakes of polymer 5 and branched polymers 6a–f.

laws and the swelling ratio of the branched membranes decreases with increasing water uptake. This may be due to the increased branching points, which limit the movement of polymer chain in water and prevent swelling of the branched membranes.

3.4. Proton conductivity and hydration number

Proton conductivities as a function of DB value were displayed in Fig. 6. The linear and branched polymers show higher proton conductivities than $10^{-2} \text{ S cm}^{-1}$, which is the lowest value of practical interest for use as PEMs in fuel cells. It is obvious that the proton conductivities increase with increasing DB value and temperature. The membrane with the highest DB value shows maximum proton conductivity up to 0.42 S cm^{-1} at 80°C , which is higher than that of Nafion 117 (0.10 S cm^{-1}) under the same conditions. It is believed that proton conductivity relies heavily on the IEC values and water uptake of electrolyte membranes. However, the IEC values slightly decrease with increasing DB value. The excellent proton conductivity may mainly be attributed to high water uptake of the electrolyte membranes. Additionally, the

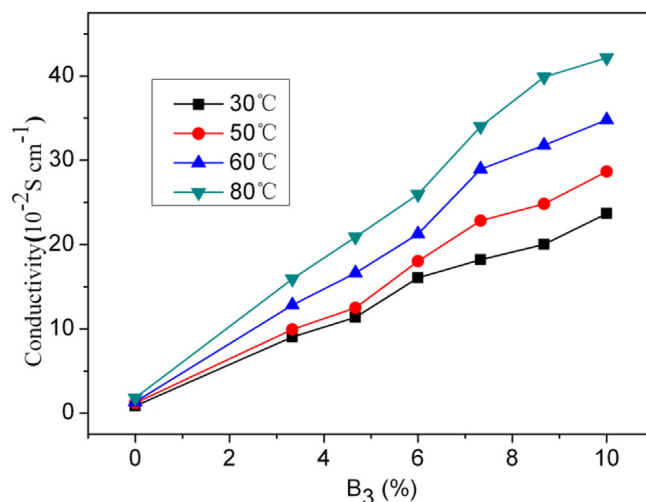


Fig. 6. Proton conductivities of polymer 5 and branched polymers 6a–f.

membrane morphology plays an important role for proton transport in PEMs. As is described in the literature [3,34], examination of these branched membranes by TEM reveals phase-separated worm-like ionic domains that are highly connected, in contrast to the dead-ended channels commonly associated with their linear analogs. Better connectivity leads to better proton conductivity and hence the branched membranes exhibit better proton conductivity than that of linear membranes in similar IEC value. As shown in Fig. 7, the linear and branched membranes exhibit Arrhenius-type temperature-dependant proton conductivity behavior. The activation energy (E_a) for proton conductivity was calculated according to Arrhenius equation:

$$\sigma = A \exp(-E_a/RT)$$

where σ is the proton conductivity (mS cm^{-1}), R is the universal gas constant ($8.314 \text{ J mol}^{-1} \text{ K}^{-1}$), A is the pre-exponential factor, and T is the absolute temperature (K). The linear membrane exhibits higher activation energy value ($13.12 \text{ kJ mol}^{-1}$) than those of the branched membranes. With increasing DB value, activation energy of the branched membranes shows a decreasing trend. The

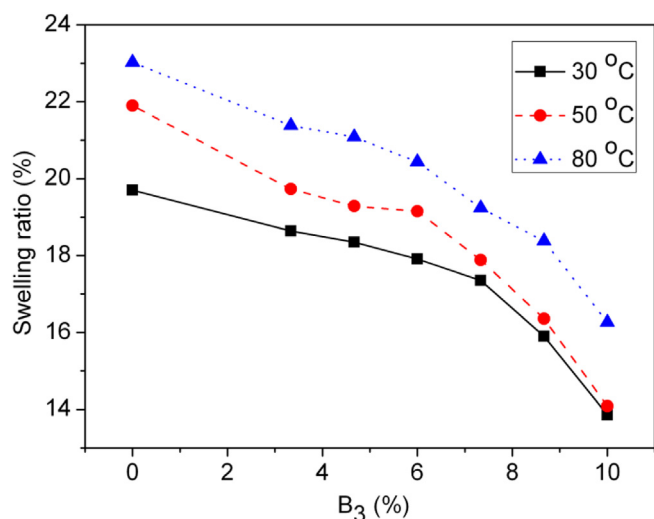


Fig. 5. Swelling ratios of polymer 5 and branched polymers 6a–f.

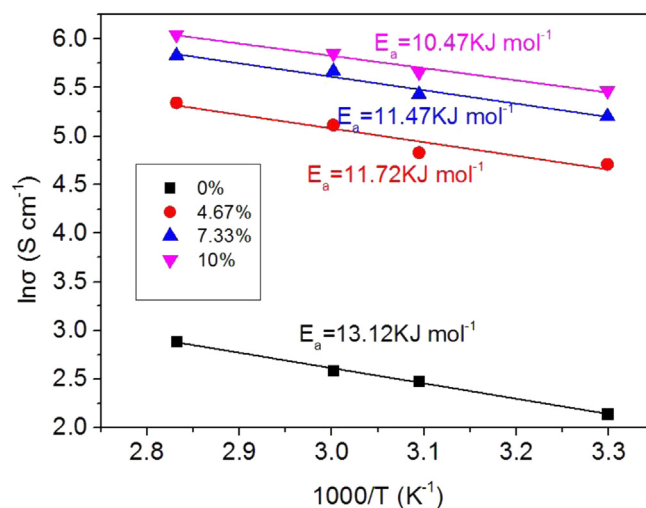


Fig. 7. The Arrhenius-type temperature-dependant proton conductivity (σ) behavior of the membranes.

membrane with the highest DB value shows the relative small activation energy value ($10.47 \text{ kJ mol}^{-1}$) close to that of Nafion 117 (9.56 kJ mol^{-1}) [42], hence allowing for high proton conductivity.

Hydration number (λ), the number of water molecules per sulfonic acid group, was calculated by combining water uptake and IEC data. The results were presented in Table 3. Although the IEC values slightly decrease with increasing DB value, we could see that λ values of the branched membranes increased remarkably with increasing DB value. Proton conductivity and λ values of the branched membranes exhibit a similar law. The λ values of the branched membranes can more directly reflect the proton conductivity, and with increasing λ values, the proton conductivities of the membranes increase remarkably.

3.5. Thermal and mechanical properties

The thermal properties of branched polymers were characterized by assessing the glass transition and decomposition temperatures from DSC and TGA, respectively. TGA experiment was carried out from 50 to 600°C at a heating rate of $10^\circ\text{C min}^{-1}$ under the protection of nitrogen. Fig. 8 shows the TGA spectra of branched sulfonated polymers. Two consecutive weight loss steps were observed in the linear and branched sulfonated polymers. The first weight loss beginning at $280\text{--}400^\circ\text{C}$ could be attributed to the weight loss of $-\text{SO}_3\text{H}$ by the desulfonation. The second weight loss over 480°C is due to the thermal decomposition of polymer main chains, in which the polymer residuals are further degraded. The glass transition temperatures (T_g) were determined on a TA instrument Q200 DSC at a heating rate of $10^\circ\text{C min}^{-1}$ under the protection of nitrogen. DSC measurement of the polymers at a temperature range from 30 to 280°C did not show glass transition temperature (T_g) during the second scan before thermal decomposition. The high T_g values of the polymers are attributed to their ionomeric nature, which is analogous to the results described in our previous publication [40]. The high glass transition and the high decomposition temperature of the sulfonated polymers indicate that these branched sulfonated polymers have the potential application for high temperature ($>100^\circ\text{C}$) PEMFC.

Mechanical properties of the PEM materials affect manufacturing condition of MEAs and the durability of PEMFC operations. The mechanical properties of the linear and branched membranes were determined at 30°C and 100% relative humidity. Table 3 lists the tensile strength of the linear and branched membranes. The resulting membranes exhibit a tensile strength of $11.5\text{--}31.2 \text{ MPa}$, while the tensile strength of Nafion 117 is 25.7 MPa [41]. Tensile strength of the linear membrane is better than these of the branched membranes. With increasing DB values, tensile strength of the branched membranes decreases slowly. This may be due to

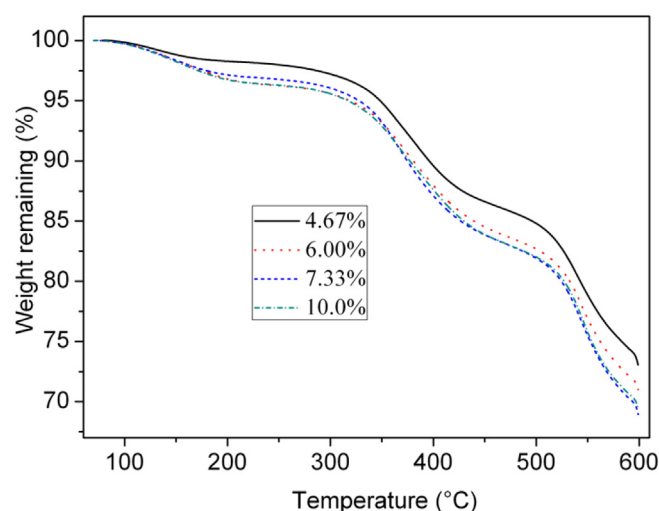


Fig. 8. TGA curves of branched polymers 6.

the introduction of branch points, which decreases the chain entanglement and thus decreases the mechanical properties of the branched membranes. Improving the tensile strength of the branched membranes may be an important problem to meet requirements for the PEMFC assembly application.

3.6. Oxidation and hydrolytic stabilities

The oxidative stability of PEMs is important for their practical applications. Proton exchange membranes are known to undergo degradation resulting from hydroxyl or peroxy free radicals formed by the decomposition of H_2O_2 generated at cathode during operational conditions of fuel cells [8,9]. Following a well-established procedure, the oxidative stability of the membranes was evaluated by measuring the elapsed time that a membrane began to break after immersion in Fenton's reagent (2 ppm FeSO_4 in 3% H_2O_2) at 80°C . The results were shown in Fig. 9. The poly(arylene ether ketone)s membrane exhibits better oxidative stabilities than those of the poly(arylene ether ketone)s membrane reported by our group [40] and the partially fluorinated branched sulfonated poly(ether ether ketone)s membrane reported by Wang' groups [37]. Similar to the case of the branched sulfonated

Table 3
Water uptake and Tensile strength of polymer 5 and branched polymers 6a–f.

	Water uptake ^a (wt%)	λ	Density ^b (g cm^{-3})	Tensile strength (MPa)
5	44.4	13.4	1.61	31.2
6a	46.5	14.4	1.59	23.3
6b	50.8	15.9	1.55	19.8
6c	52.7	16.5	1.37	18.0
6d	56.0	17.9	1.31	17.0
6e	61.8	20.0	1.23	14.6
6f	65.7	21.3	1.10	11.5
Nafion 117	19 ^c	NR ^d	1.98 ^c	25.7 ^c

^a Measured at 30°C .

^b Based on dry state.

^c Data taken from Ref. [41].

^d Not reported.

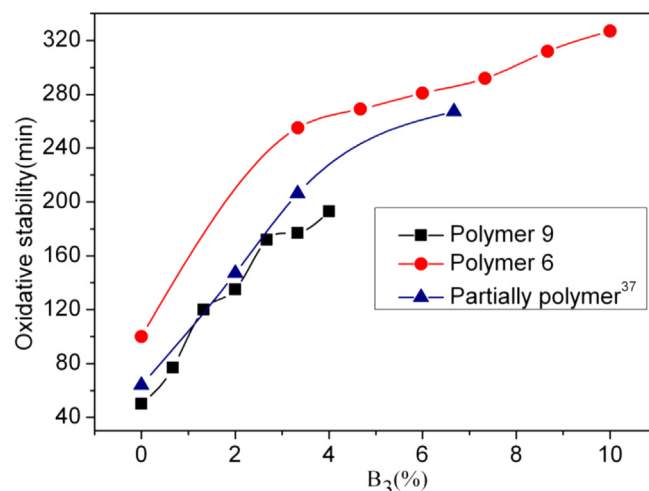


Fig. 9. Oxidative stability of membranes.

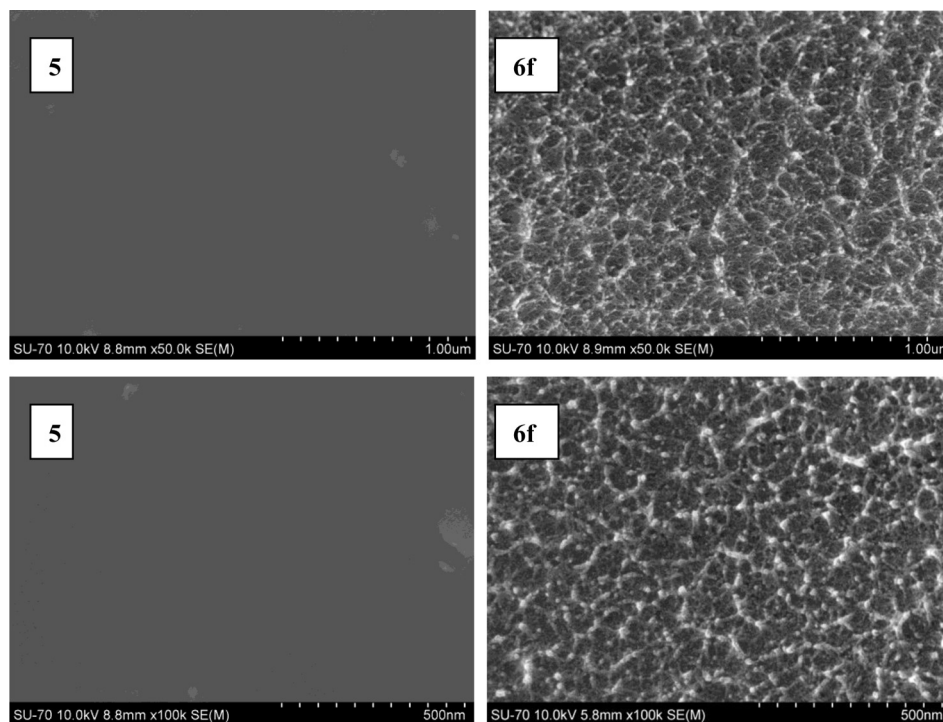


Fig. 10. Cross-section SEM images of linear membrane **5** and branched membrane **6f**.

poly(arylene ether ketone)s membranes reported [40], oxidative stability of the branched sulfonated poly(arylene ether ketone sulfone)s membranes increases with increasing DB values. The membrane formed by the branched polymers with 10 mol% B₃-3 shows the best oxidative stability and the elapsed time is 327 min, which is 3.27 times longer than that of the membrane formed by linear polymers (100 min) at the same condition. The hydrolytic stability was also investigated by treating the membrane samples in boiling water for more than 8 days. The membranes did not change in shape and appearance after the treatment, implying that there was no hydrolysis occurred during the treatment.

3.7. Membrane density and microstructure

These results of the density were compiled in Table 3. The densities of the branched membranes decrease with increasing DB values. This is mainly due to the increase of branching points in the

membranes. With increasing branching points, free volume of the branched polymer membranes increase, which leads to the decrease in the density of the membranes. The free volume can also help trap water leading to the significant increase of water uptake.

The microstructure of the linear and branched membranes (**5**, **6e** and **6f**) was investigated by SEM and the cross-section images were shown in Fig. 10. The cross-section of linear membrane **5** is dark with smooth surface. It is because the linear polymer chain is flexible and can be easy to arrange together freely, which can induce compact structure and high density of the linear membranes. From the cross-section images of the branched membrane **6f**, it could be obviously found that the rigid net-work structure is formed because of the branch points with hard arms and the short chain between the branching points. The special microstructure of **6f** results in the increase of free volume in membrane, as a result, the density of branched membrane will decrease and water uptake and hydration number will increase. The phase morphology of

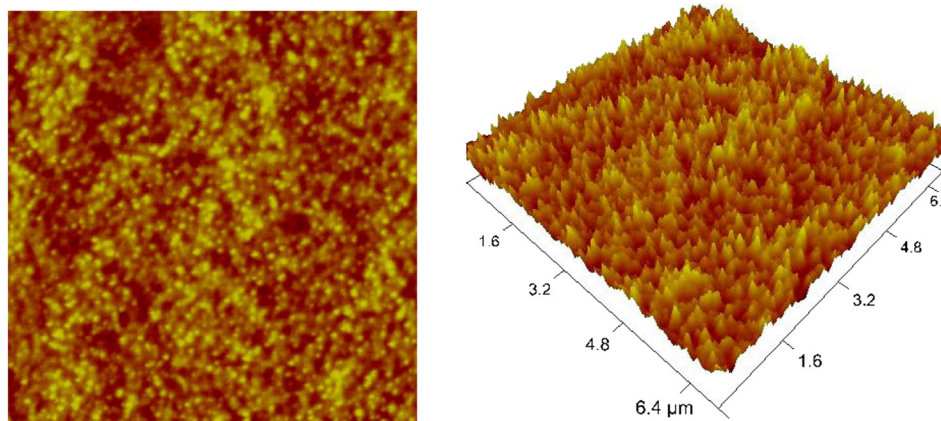


Fig. 11. Cross-section 2D (700 nm × 700 nm) and 3D (700 nm × 700 nm × 350 nm) AFM images of branched membrane **6f**.

branched membranes **6f** was also investigated by AFM and the results were illustrated in Fig. 11. The AFM images also presented a bright/dark nanophase separated morphology [43]. The hydrophilic domain of the branched membrane **6f** is highly connected, which induces better proton conductivity than the linear analogs.

4. Conclusion

Highly branched nonfluorinated sulfonated poly(fluorenyl ether ketone sulfone)s were successfully prepared by polycondensation from sulfonated 4,4'-difluorobenzophenone, bisphenol fluorene, 1,3,5-tris(4-(4-fluorophenylsulfonyl)phenyl) benzene and 4,4'-difluorodiphenyl sulfone. The B₃-3 scaffold with long and hard arms can reduce cross-linked opportunities of the branched polymers and improve DB value. The resulted polymers could be cast into transparent, flexible, and tough membranes. With increasing DB value, water uptake, proton conductivity and oxidative stability of the branched membranes increase, while swelling ratio and mechanical properties of the branched membranes decrease. The membrane with the highest DB value (10%) exhibits considerable proton conductivity (0.42 S cm⁻¹) and oxidative stability (327 min), as well as relatively low swelling ratio (16.2%) at 80 °C.

Acknowledgments

The authors would like to thank the National Natural Science Foundation of China, China (Nos. 51003060, 51171117 and 51101103) and Shenzhen Sci & Tech research grant (JC2011042 100070A and ZYC201105170225A) for their financial support.

Appendix A. Supplementary data

Supplementary data related to this article can be found at <http://dx.doi.org/10.1016/j.jpowsour.2014.03.064>.

References

- [1] B. Bae, T. Yoda, K. Miyatake, H. Uchida, M. Watanabe, *Angew. Chem. Int. Ed.* 49 (2010) 317–320.
- [2] M.A. Hickner, H. Ghassemi, Y.S. Kim, B.R. Einsla, J.E. McGrath, *Chem. Rev.* 104 (2004) 4587–4611.
- [3] T.J. Peckham, S. Holdcroft, *Adv. Mater.* 22 (2010) 4667–4690.
- [4] H. Zhang, P.K. Shen, *Chem. Rev.* 112 (2012) 2780–2832.
- [5] T. Higashihara, K. Matsumoto, M. Ueda, *Polymer* 50 (2009) 5341–5357.
- [6] B.P. Tripathi, V.K. Shahi, *Prog. Polym. Sci.* 36 (2011) 945–979.
- [7] H. Hou, M.L. Di Vona, P. Knauth, *J. Membr. Sci.* 423 (2012) 113–127.
- [8] R. Borup, J. Meyers, B. Pivovar, Y.S. Kim, R. Mukundan, N. Garland, D. Myers, M. Wilson, F. Garzon, D. Wood, P. Zelenay, K. More, K. Stroh, T. Zawodzinski, J. Boncella, J.E. McGrath, M. Inaba, K. Miyatake, M. Hori, K. Ota, Z. Ogumi, S. Miyata, A. Nishikata, Z. Siroma, Y. Uchimoto, K. Yasuda, K.-i. Kimijima, N. Iwashita, *Chem. Rev.* 107 (2007) 3904–3951.
- [9] H. Zhang, P.K. Shen, *Chem. Soc. Rev.* 41 (2012) 2382–2394.
- [10] A. Iulianelli, A. Basile, *Int. J. Hydrogen Energy* 37 (2012) 15241–15255.
- [11] J. Lawrence, T. Yamaguchi, *J. Membr. Sci.* 325 (2008) 633–640.
- [12] A. El-Kharouf, A. Chandan, M. Hattenberger, B.G. Pollet, *J. Energy Inst.* 85 (2012) 188–200.
- [13] B.J. Liu, G.P. Robertson, D.S. Kim, M.D. Guiver, W. Hu, Z.H. Jiang, *Macromolecules* 40 (2007) 1934–1944.
- [14] J. Miyake, M. Watanabe, K. Miyatake, *ACS Appl. Mater. Interfaces* 5 (2013) 5903–5907.
- [15] L. Wang, Y.Z. Meng, X.H. Li, M. Xiao, S.J. Wang, A.S. Hay, *J. Membr. Sci.* 280 (2006) 108–115.
- [16] Y.L. Liu, *Polym. Chem.* 3 (2012) 1373–1383.
- [17] S. Takamuku, P. Jannasch, *Macromolecules* 45 (2012) 6538–6546.
- [18] E.A. Weiber, S. Takamuku, P. Jannasch, *Macromolecules* 46 (2013) 3476–3485.
- [19] N. Li, S.Y. Lee, Y.-L. Liu, Y.M. Lee, M.D. Guiver, *Energy Environ. Sci.* 5 (2012) 5346–5355.
- [20] B. Bae, K. Miyatake, M. Uchida, H. Uchida, Y. Sakiyama, T. Okanishi, M. Watanabe, *ACS Appl. Mater. Interfaces* 3 (2011) 2786–2793.
- [21] A.K. Mohanty, E.A. Mistri, A. Ghosh, S. Banerjee, *J. Membr. Sci.* 409 (2012) 145–155.
- [22] L. Wang, S. Xiang, G. Zhu, *Chem. Lett.* 38 (2009) 1004–1005.
- [23] X. Zhang, L. Sheng, T. Hayakawa, M. Ueda, T. Higashihara, *J. Mater. Chem. A* 1 (2013) 11389–11396.
- [24] L. Wang, G.M. Zhu, J.Q. Li, C.M. Gao, *Polym. Bull. (Berlin)* 66 (2011) 925–937.
- [25] K.-S. Lee, M.-H. Jeong, J.-P. Lee, J.-S. Lee, *Macromolecules* 42 (2009) 584–590.
- [26] F.C. Ding, S.J. Wang, M. Xiao, Y.Z. Meng, *J. Power Sources* 164 (2007) 488–495.
- [27] J.A. Kerres, *Fuel Cells* 5 (2005) 230–247.
- [28] S.J. Wang, Y. Chen, M. Xiao, Y.Z. Meng, *J. Appl. Polym. Sci.* 127 (2013) 1981–1988.
- [29] H.S. Dang, D. Kim, *Int. J. Hydrogen Energy* 37 (2012) 19007–19016.
- [30] H.-S. Dang, D. Kim, *J. Power Sources* 222 (2012) 103–111.
- [31] S. Gao, C. Zhao, H. Na, *J. Power Sources* 214 (2013) 285–291.
- [32] X. Chen, P. Chen, Z. An, K. Chen, K. Okamoto, *J. Power Sources* 196 (2011) 1694–1703.
- [33] K. Matsumoto, T. Higashihara, M. Ueda, *Macromolecules* 41 (2008) 7560–7565.
- [34] S. Matsumura, A.R. Hlil, C. Lepiller, J. Gaudet, D. Guay, Z. Shi, S. Holdcroft, A.S. Hay, *Macromolecules* 41 (2008) 281–284.
- [35] H.S. Park, D.W. Seo, S.W. Choi, Y.G. Jeong, J.H. Lee, D. Il Kim, W.G. Kim, *J. Polym. Sci. Part A Polym. Chem.* 46 (2008) 1792–1799.
- [36] Y. Chikashige, Y. Chikyu, K. Miyatake, M. Watanabe, *Macromol. Chem. Phys.* 207 (2006) 1334–1343.
- [37] Y. Li, M. Xie, X. Wang, D. Chao, X. Liu, C. Wang, *Int. J. Hydrogen Energy* 38 (2013) 12051–12059.
- [38] W. Guo, X. Li, H. Wang, J. Pang, G. Wang, Z. Jiang, S. Zhang, *J. Membr. Sci.* 444 (2013) 259–267.
- [39] L. Wang, K. Li, G. Zhu, J. Li, *J. Membr. Sci.* 379 (2011) 440–448.
- [40] L. Wang, D. Wang, G. Zhu, J. Li, *Eur. Polym. J.* 47 (2011) 1985–1993.
- [41] D.S. Kim, Y.S. Kim, M.D. Guiver, B.S. Pivovar, *J. Membr. Sci.* 321 (2008) 199–208.
- [42] E.A. Mistri, A.K. Mohanty, S. Banerjee, H. Komber, B. Voit, *J. Membr. Sci.* 441 (2013) 168–177.
- [43] J.Y. Chu, A.R. Kim, K.S. Nahm, H.-K. Lee, D.J. Yoo, *Int. J. Hydrogen Energy* 38 (2013) 6268–6274.